University of Baghdad
College of Engineering
JOURNAL OF ENGINEERING

Journal of Engineering
journal homepage: www.joe.uobaghdad.edu.iq
Number 7 Volume 28 July 2022

Mechanical and Energy Engineering

Conjugate Heat Transfer of Laminar Air Flow in Rectangular Mini Channel

Ali M. Aljelawy*
Ph.D. student
University of Technology
Baghdad, Iraq
engaljelawy@gmail.com

Amer M. Aldabbagh
Assist. Prof
University of Technology
Baghdad, Iraq
Aamermajeed@yahoo.com

Falah F. Hatem
Assist. Prof
University of Technology
Baghdad, Iraq
falahhatem59@yahoo.com

ABSTRACT

Conjugate heat transfer has significant implications on heat transfer characteristics, particularly in thick wall applications and small diameter pipes. In this study, a three-dimensional numerical investigation was carried out using commercial CFD software "ANSYS FLUENT" to study the influence of conjugate heat transfer of laminar flow in mini channels at constant heat flux wall conditions. Two parameters were studied and analyzed: the wall thickness and thermal conductivity and their effect on heat transfer characteristics such as temperature profile and Nusselt number. Thermal conductivity of (0.25, 10, 202, and 387) W/m^{2}C and wall thickness of (1, 5, and 50) mm were used for a channel of (1*2) mm cross-sectional dimensions. Taking the Reynolds number 800 for all cases. The results demonstrate that the conjugate conduction impact is observed at high conductivities and for large wall thicknesses in the studied materials. This impact flattened the wall temperature distribution along the channel wall instead of being an augmented linear profile. Also, it flattens the local Nusselt number due to the axial heat conduction along the walls. It reduces the effect of the entrance region of high Nusselt number while making the fluid temperature profile curved and redistributing the wall heat flux and accumulating it toward the leading edge. A decrease was observed in the average Nusselt number of 8% when increasing wall thickness from 1 mm to 50 mm for the same thermal conductivity of 10 W/m^{2}C, while an increase in Nusselt number of 19% with thermal conductivity changes from 0.25 W/m^{2}C to 10 W/m^{2}C.

Keywords: Heat transfer; conjugate; mini channel; conduction-convection; CFD

انتقال الحرارة المتزامن لجريان طباقي خلال مجرى ذو ابعاد ملمترية

*** علي محمد الجيلاوي**
طالب دكتوراه
الجامعة التكنولوجية

فلاح فاخر حاتم
استاذ مساعد
الجامعة التكنولوجية

عامر مجيد الدباغ
استاذ مساعد
الجامعة التكنولوجية

الخلاصة

على الرغم من حقيقة أن نقل الحرارة بالتوصيل المتقارن له آثار كبيرة على خصائص نقل الحرارة ، لا سيما في تطبيقات الجدران السميكة ، إلا أنه نادرًا ما يؤخذ بنظر الاعتبار. في هذه الدراسة تم إجراء دراسة نظرية ثلاثية الأبعاد باستخدام البرنامج التجاري

*Corresponding author
Peer review under the responsibility of University of Baghdad.
https://doi.org/10.31026/j.eng.2022.07.02

Article received: 11/1/2022
Article accepted: 24/3/2022
Article published: 1/7/ 2022

"*ANSYS FLUENT*" لدراسة تأثير انتقال الحرارة بالتوصيل المترافق للجريان الطباقي في القنوات الصغيرة في حالة التدفق الحراري المنتظم على الجدار. تم دراسة وتحليل معاملين هما سماكة الجدار والتوصيل الحراري وتأثيرهما على خصائص انتقال الحرارة مثل توزيع درجة الحرارة ورقم نسلت. استخدمت الموصلية الحرارية (0.25 ، 10 ، 202 ، 387) واط / م 2 كلفن وسماكة جدار (1 ، 5 ، 50) ملم لقناة بأبعاد مقطعية عرضية (1 * 2) ملم. أخذ رقم رينولدز 800 لجميع الحالات. أظهرت النتائج أن تأثير التوصيل المقترن لوحظ في الموصلية العالية ولسمك الجدار الكبير في المواد المدروسة. وكان هذا التأثير يعمل على تسطيح شكل توزيع درجة حرارة الجدار على طول جدار القناة بدلاً من كونه يتزايد خطيًا وأيضًا يعمل على تسطيح رقم *Nusselt* المحلي بسبب التوصيل الحراري المحوري على طول الجدران ويقلل من تأثير منطقة الدخول ذات رقم *Nusselt* العالي ، مع تقويس شكل توزيع درجة حرارة المائع ويعيد توزيع تدفق حرارة الجدار وتجميعه باتجاه الحافة الأمامية . حيث لوحظ انخفاض في متوسط عدد *Nusselt* بنسبة 8٪ عند زيادة سمك الجدار من 1 مم إلى 50 مم لنفس الموصلية الحرارية بمقدار 10 وات / م 2 ، بينما زيادة في عدد *Nusselt* بنسبة 19٪ مع تغير التوصيل الحراري من 0.25 وات / م 2. إلى 10 وات / م 2 درجة مئوية.

الكلمات الرئيسية: انتقال حرارة، متزامن، قنوات صغيرة، توصيل-حمل،CFD

1. INTRODUCTION

Certain heat transfers require the use of thick-walled tubes and the flow of heat into them. Convection not only transfers heat in this scenario, but the conduction impact can also be significant on the solid and possibly on the liquid sides. This phenomenon is referred to as conjugated heat transfer, and it has been the topic of several decades of numerical and computer analysis attempts. Although there is a vast amount of literature, the following are a few current works.

(Khalesi and Sarunac, 2019) performed a numerical analysis of the developing laminar flow and conjugate heat transfer in a rectangular micro-channel for supercritical CO_2 and liquid sodium as working fluids. Numerical results showed that large variations in CO_2 properties in the critical and pseudo-critical regions affect the flow and heat transfer. Also, in the fully-developed region, the local values of wall shear stress and heat transfer coefficient are not constant but are strong functions of the local heat flux at the solid-fluid interface, which varies due to large variation in sCO2 properties. **(Varol, et al., 2008)** investigated the combined heat transfer and natural convection of various vertical walls. The authors concentrated on the formation of entropy as a result of conjugated heat transport. Entropy production during heat transfer has been found to be greater since the fluid flow is not reversed. It appears as though natural convection-based heat transmission has become more prevalent in recent years than forced convection-based heat transfer. **(Kuznetsov and Sheremet, 2010)** carried out a numerical analysis of turbulent natural convection in terms of conjugated heat transfer caused by the thick wall envelope. They set out to define the thermal state, which is very difficult. With wall pillars, the k standard was employed. A Grashof number between 108 and 1010 was used as a separate parameter. They gave data comparable to those found in the literature to demonstrate the validity of their work. Then they could assess the impact of the criteria they've chosen. They concluded by presenting a link between Nusselt and Graschoff's numbers. Like natural convection, another significant search area for conjugated heat transfer is the DNS of conjugated heat transfer. **(Tiselj and Cizelj, 2012)** reported on DNS for turbulent channel flow with conjugated heat transfer at a Prandtl number (Pr) 0.01. Additionally, the condition of the variable temperature boundary, as well as the condition of the constant temperature boundary, was explored. The particular Pr value was proportional to the amount of liquid that came into contact with the sodium steel. It has been demonstrated that turbulent temperature variations can impact the distribution of wall temperatures. **(Satish and Venkatasubbaiah, 2016)** conducted a similar study, where the flow is contained between two flat plates; however, one of the panels was moving. They reported that thermal conduction through a wall modifies the heat transfer parameters dramatically. While their primary conclusions were

predictable, they emphasized the need to improve heat transfer by raising the speed of the moving plate. Additionally, they employed the k-turbulent model. **(Canli, et al., 2018)** presented temperature distribution results of ANSYS CFD using simple and coupled pressure velocity coupling for a thick-walled plain circular pipe and turbulent flow inside it. **(Hajmohammadi *et al.*, 2014)** presented a paper dealing with the optimized laminar forced convection heat transfer inside a rectangular duct where the outer surfaces were exposed to a fixed overall heat load but variable heat flux distribution. Because the overall heat load was considered fixed, optimizing heat transfer was indicated by minimizing maximum temperature. **(Joneydi Shariatzadeh, 2016)** developed an analytical solution for conjugating turbulent forced boundary layer flow over plates. The paper presented a semi-analytical solution based on the differential transformation method. This method was used to solve the problem's nonlinear differential equation. The author noted a little change in temperature between the conjugated and unconjugated cases. **(Karvinen, 1978)** considered convective heat transfer over a flat plate using forced convection. The results of the analytical analysis were compared to experimental measurements. **(Malvandi, et al., 2015)** demonstrated an attempt to analyze conjugate heat transfer from a flat plate contained in a nanofluid flow field. The turbulent laminar transition was resented during the RANS evaluation of the conjugate heat transfer scenario. **(Abdollahzadeh *et al.*, 2017)** investigated the performance of eight distinct turbulence models was discussed. Additionally, they included additional parameters in the study, such as tilt angle, Richardson number, and position of the transition point. **(Al-Zaharnah, et al., 2000)** presented a study in which fully developed laminar flow through a pipe was considered. Uniform heat flux from the external surface of the pipe was introduced. The thermal stresses developed due to conjugate heating were analyzed. The governing flow and energy equations were solved numerically using a control volume approach. Thermal stresses due to temperature gradient were also computed. Various fluids and thermal conductivity ratios were taken into account. This helps to examine the effect of the thermal properties of fluid and pipe on the resulting stresses. It was found that the low Prandtl number and low thermal conductivity ratios resulted in almost uniform radial temperatures and low radial effective stresses. **(Kokugan *et al.*, 1975)** performed an experiment in which the wall temperature of a heated vertical open tube was maintained constant. Mechanical energy balances in tubes had been used to derive Grashof-Reynolds number correlations. According to available numerical results, the findings were in good agreement with the results.

According to **(Mohammed and Salman, 2007)**, a vertical circular pipe with different inlet configurations: cylindrical pipes of different lengths, sharp-edge, and bell-mouth, was subjected to extensive experimental data. It was demonstrated that the inlet conditions and configurations significantly impacted the heat transfer results. The computational model developed by these authors **(Mohammed and Salman, 2008)** had been validated through comparisons with their own experimental data. The radial and axial heat conductivity and thermal stresses in a pipe with uniform or non-uniform wall heat flux of fully developed laminar forced convective conjugate heat transfer were examined by **(Yapici and Albayrak, 2004)**. The finite difference method was used to conduct the two-dimensional steady-state analysis. The temperature and stress ratio distributions inside the pipe wall have been shown for heat fluxes applied uniformly and non-uniformly from the outer surface for two different mean flow velocities. Temperature patterns in the pipe's flow were presented in all of the examined cases. **(Arici and Aydin, 2009)** made a numerical investigation of thermally developing laminar forced convection in a pipe, including viscous dissipation and wall conductance. On the outer surface of the pipe wall, constant heat flux was assumed. The finite volume method was employed. The distributions of the developing temperature and local Nusselt number in the entry region were obtained. The relation between the Brinkman number and the dimensionless thermal conductivity was clarified. The heat transfer

properties of a thin vertical strip with internal heat generation were examined at a steady state by **(Méndez and Treviño, 2000)**. **(Bilir, 2002)** presented a study using the finite difference method to investigate an unsteady conjugate heat transfer problem in a thermally developing laminar pipe flow. **(Merkin and Pop, 1996)** performed a numerical investigation using the finite difference method to investigate the dimensionless governing equations for conjugate free convection boundary layer flow on a horizontal plate. **(He *et al.*, 2020)** The flow and conjugate heat transfer characteristics of double-wall cooling were analyzed numerically, which had a film plate with gradient thickness for gas turbine cooling. The gradient thickness along the flow direction was realized by setting the angle (α) between the lower surface of the film plate and the horizontal plane at −1.5 deg and 1.5 deg respectively. The results showed that the thickening of the film plate downstream was beneficial to improve overall cooling effectiveness at low blowing ratio, and the ability of improvement downstream decreased as the initial film plate thickness increases, which was due to the increase of heat transfer resistance

Advanced analysis of thermal behavior of three-dimensional conjugate heat transfer in a horizontal pipe with a fluid flow in steady and transient states was performed by **(Ajeena and Al-Madhhachi, 2020)**. A numerical procedure of three-dimensional conjugate heat conduction in a solid wall and heat convection in a laminar flow with radial radiation was developed by analyzing computational modeling of the solid-fluid domains. The procedure was based on the assumption that the gradient of temperature and heat flux of the solid-fluid domains was dependent on the thermal equivalent between conduction, convection, and radiation heat transfers. They concluded that the heat flux distribution of the solid pipe was noticeably non-uniform in the transient condition but uniform in a steady-state condition. In contrast, the temperature distribution was the opposite, where it was non-uniform at steady-state and uniform for transient conditions.

It is obvious from the literature that the conjugate heat transfer in mini channels hasn't been well investigated. So in this study, a numerical investigation was carried out to study the effect of conjugate heat transfer of laminar flow forced convection in a rectangular mini channel using commercial CFD software. Because it is expected that the effect of conjugate heat transfer through the small channel will be large. Incidentally, this study was inspired by the idea of developing a unique heat exchanger type, the printed circuit heat exchanger (PCHE). It is a type of plate heat exchanger of mini channels size.

2. NUMERICAL WORK

2.1 Computational domain

The computational domain consists of a single rectangular channel of dimensions (2*1) mm with a length of 500 mm. Still, half of this domain was simulated using the symmetry option to reduce the time consumption, so the domain becomes of square cross-section (1*1) mm with boundary conditions stated in **Fig. 1**. A structured grid was used to mesh the domain with three prism layers near the walls, as shown in **Fig. 2**.

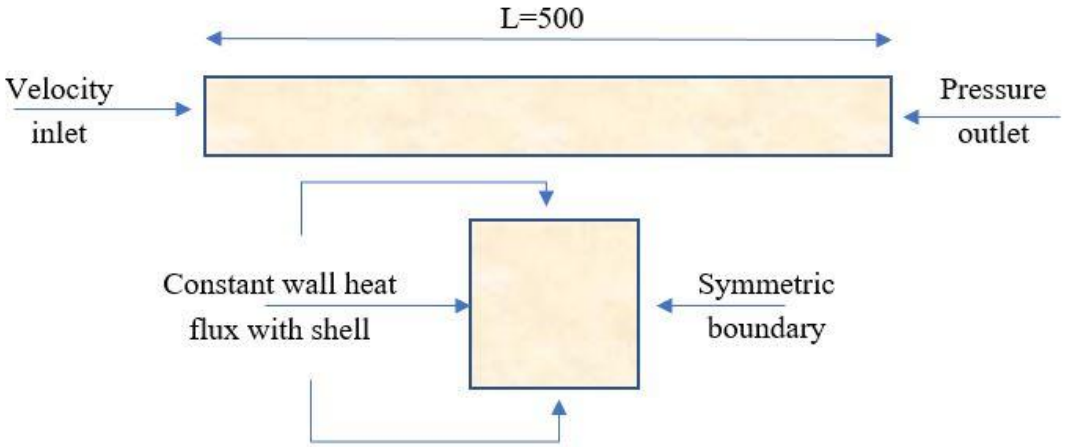

Figure 1. Geometry front and side view with boundary conditions used.

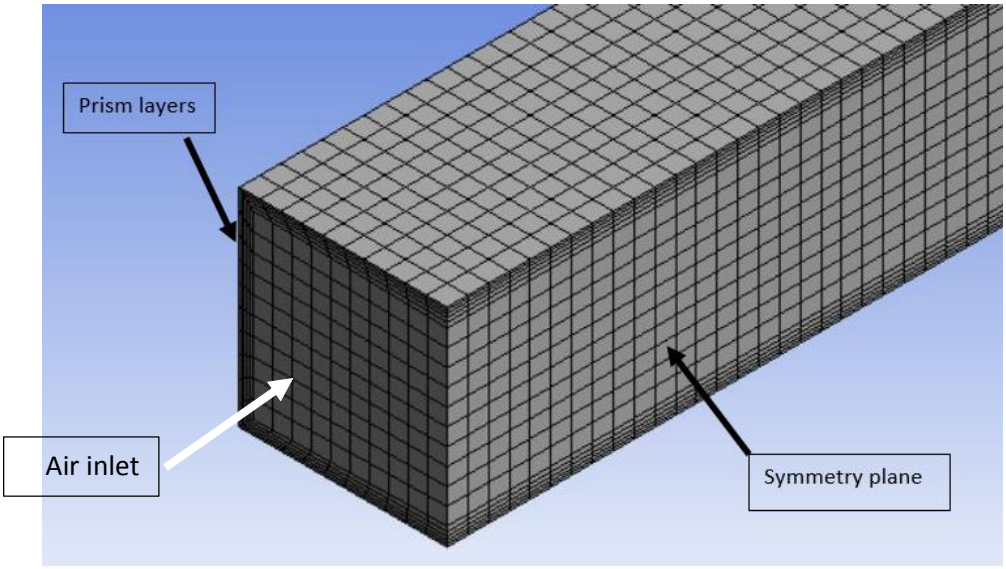

Figure 2. Mesh of channel model with boundary conditions.

2.2 Governing equations and boundary conditions

The commercial software ANSYS FLUENT 18.0 is employed for solving the governing equations of continuity, momentum, and energy. They are listed as follows

Continuity

$$\frac{\partial u}{\partial x}+\frac{\partial v}{\partial y}+\frac{\partial w}{\partial z}=0$$

Momentum x- component:

$$\rho\left(\frac{\partial u}{\partial t}+u\frac{\partial u}{\partial x}+v\frac{\partial u}{\partial y}+w\frac{\partial u}{\partial z}\right)=-\frac{\partial p}{\partial x}+\mu\left(\frac{\partial^2 u}{\partial x^2}+\frac{\partial^2 u}{\partial y^2}+\frac{\partial^2 u}{\partial z^2}\right)+\rho g_x$$

Momentum y - component:

$$\rho\left(\frac{\partial v}{\partial t}+u\frac{\partial v}{\partial x}+v\frac{\partial v}{\partial y}+w\frac{\partial v}{\partial z}\right)=-\frac{\partial p}{\partial y}+\mu\left(\frac{\partial^2 v}{\partial x^2}+\frac{\partial^2 v}{\partial y^2}+\frac{\partial^2 v}{\partial z^2}\right)+\rho g_y$$

Momentum z - component:

$$\rho\left(\frac{\partial w}{\partial t}+u\frac{\partial w}{\partial x}+v\frac{\partial w}{\partial y}+w\frac{\partial w}{\partial z}\right)=-\frac{\partial p}{\partial z}+\mu\left(\frac{\partial^2 w}{\partial x^2}+\frac{\partial^2 w}{\partial y^2}+\frac{\partial^2 w}{\partial z^2}\right)+\rho g_z$$

Energy equation

$$\rho C_p\left(u\frac{\partial T}{\partial x}+v\frac{\partial T}{\partial y}+w\frac{\partial T}{\partial z}\right)=k\left(\frac{\partial^2 T}{\partial x^2}+\frac{\partial^2 T}{\partial y^2}+\frac{\partial^2 T}{\partial z^2}\right)$$

To solve these equations, boundary conditions are needed, so the three-dimensional x,y, and z boundary conditions in the non-dimensional form are:

First of all, the non-dimensional parameters are described as follows:

$Z=z/L$, $Y=y/H$, $X=x/W$

$U=u/u_{in}$, $V=v/u_{in}$, $W=w/u_{in}$

Where :

L: length of the channel

H: height of the channel

W: width of the channel

So, for momentum boundary conditions

At Y=0 and Y=1	U=V=W=0	no slip condition
At X=0	U=V=W=0	no slip condition
At X=0.5	$\partial U/\partial Y = 0$, $\partial V/\partial Y = 0$ and W=0	symmetry
At Z=0	U=V=0 , and W= 1	inlet velocity
At Z=1	$p_{abs}=p_{static}+p_{operating}$, $p_{static}=0$	U,V and W are extrapolated

(Carlson, 2011)

While, for thermal boundary conditions

At Y=0 and Y=1	$q=-k\partial T/\partial Y$	wall heat flux
At X=0	$q=-k\partial T/\partial X$	wall heat flux
At X=0.5	$\partial T/\partial X=0$	symmetry
At Z=0	T=Ti	inlet temperature
At Z=1	$p_{static}=0$,	temperatures are extrapolated

2.3 Computational setup

The assumptions used here are steady-state, laminar flow, uniform velocity, and negligible viscous dissipation and radiation effects. Air was used as the working fluid with constant fluid properties. Constant heat flux was applied at the walls except for one wall, which was the symmetry wall. All the cases were simulated at Re=800. By enabling the shell conduction option at the wall, there was no need to mesh the wall thickness and thus reduce the computational time. Different wall thickness was used (1, 5, and 50) mm and thermal conductivity (0.25, 10, 202, and 387) W/m^2C. The segregated solver was used for solving the governing equations with double precision for higher accuracy. Residuals were set at 10^{-4} for continuity and 10^{-6} for others, and monitoring of

the required parameters was performed. A grid-independent test was carried out for the average Nusselt number for the case of k=387 and 1mm thickness, as shown in **Table 1**. All of this work was to ensure the result's accuracy.

Table 1. Mesh independent test results.

Cell number	Nu
501211	3.772
1106580	3.979
2079760	3.983

2.3 Data reduction

The heat transfer coefficient was calculated using the local average at sections because the conjugate heat transfer cause redistributes the heat flux at the wall

$$h_i = \frac{q_i''}{T_{\text{bulk}} - T_{\text{wall}}}$$

$$Nu_i = \frac{h_i \, d_h}{k_f}$$

$$d_{\text{h}} = \frac{4A}{\text{P}}$$

Where qi'' is the local average heat flux at a section, T_{wall} is the wall temperature and, T_{bulk} is the average bulk air temperature which is mass-weighted average temperature. Nu_i represents the local average Nusselt number, d_{h} is the hydraulic diameter.

There is no need to perform a case for validation; one of the cases could be validated, for example, the case which shows the behavior of constant heat flux with the reference one in books. The validation was done for the case of low thermal conductivity and small thickness with the empirical value of fully developed laminar flow Nusselt number at constant heat flux at the walls for rectangular channels, which is a constant of 4.123 **(Holman, J.P., 2010)**, as shown in **Fig. 3**.

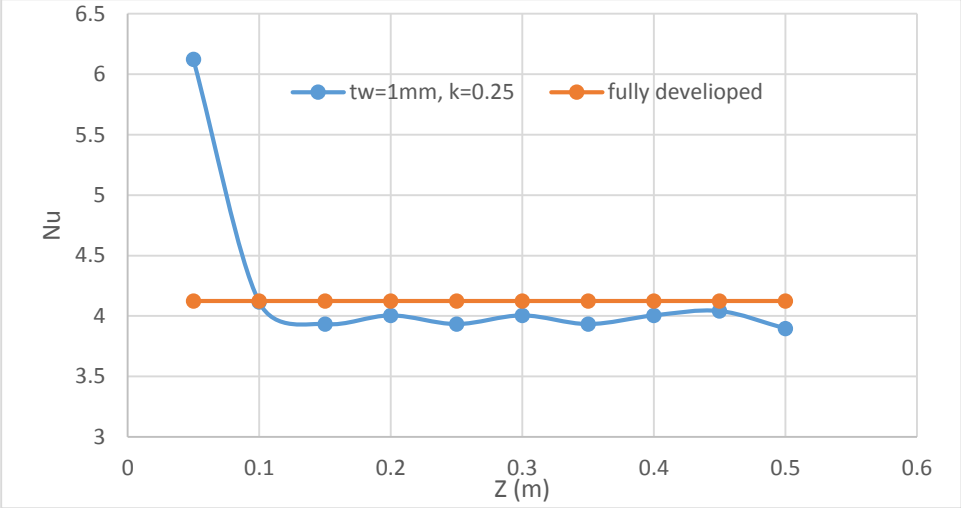

Figure 3: Validation results of local Nusselt number with the fully developed constant value

RESULTS AND DISCUSSION

Wall and air temperature, heat flux, and Nusselt number distribution along the length of the channels were plotted and analyzed

3.1 Wall and air temperature

The temperature profile shape along the channel length swings from the standard profile at constant heat flux to that at constant wall temperature. The influence of wall thickness (tw) and thermal conductivity is shown in the figures below.

Fig. 4 shows the influence of thermal conductivity on the temperature profile; it is obvious from the figures the profiles transition from the standard temperature profile of constant heat flux at low thermal conductivity to that of constant wall temperature. The conjugate plays as a balancer or flattener to the wall temperature

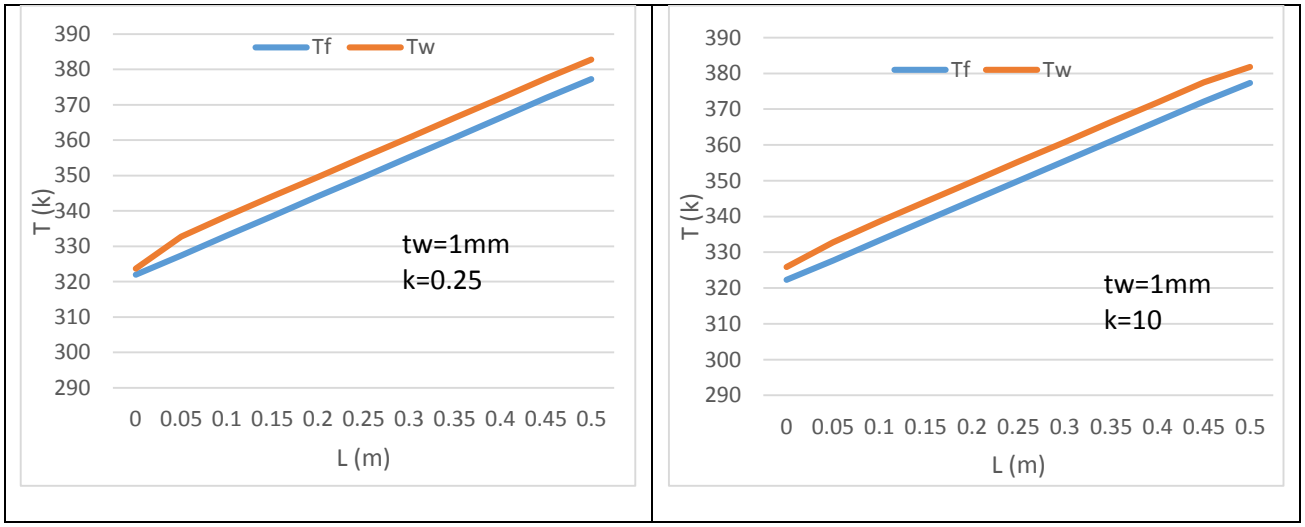

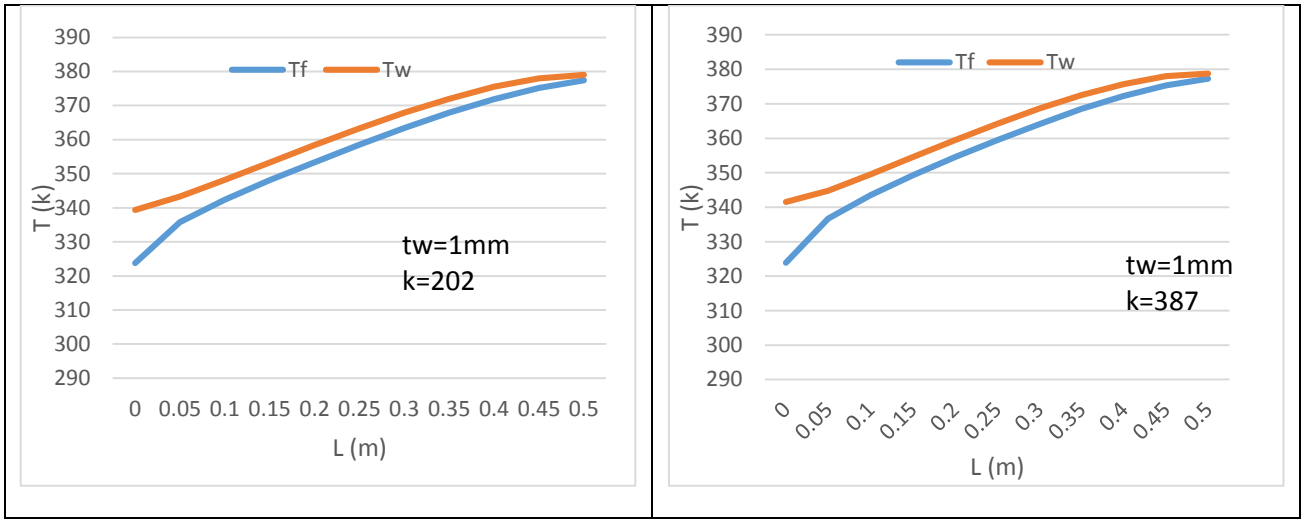

Figure 4. Temperature profile along the channel length with different thermal conductivities (0.25, 10, 202, and 387) W/m^{2}C with the same wall thickness of 1mm

Fig. 5 shows the influence of wall thickness on the temperature profile along the channel length. It shows that the higher the thickness is, the higher the conjugate impact. It is obvious from the figures the flattening of wall temperature with the high thickness. The reason behind that wall temperature flattening is the conjugate heat transfer toward the leading edge of the channel.

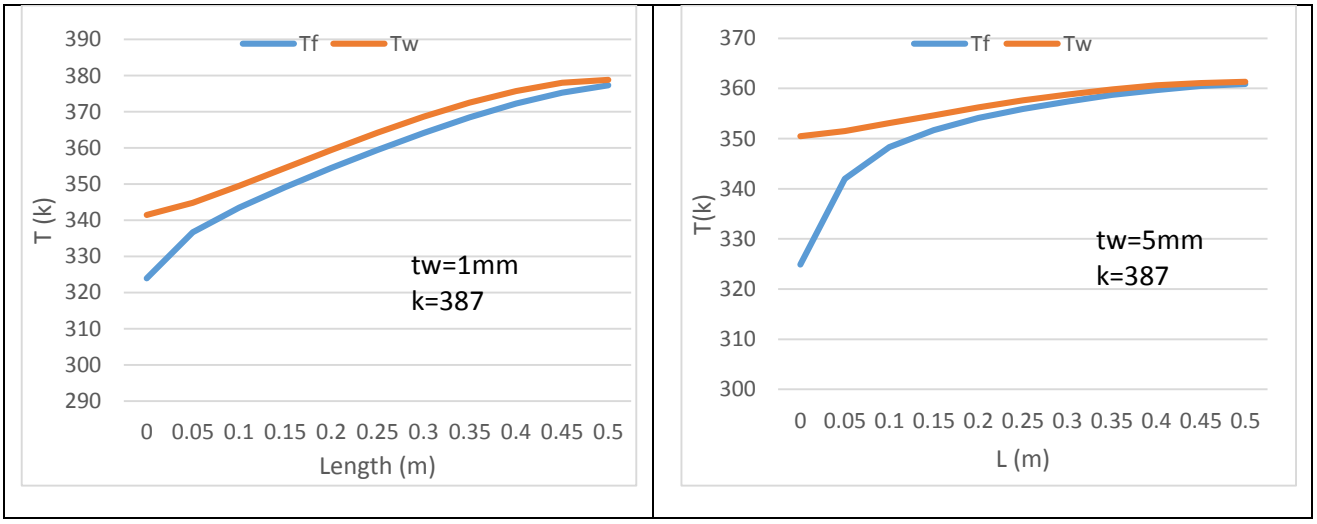

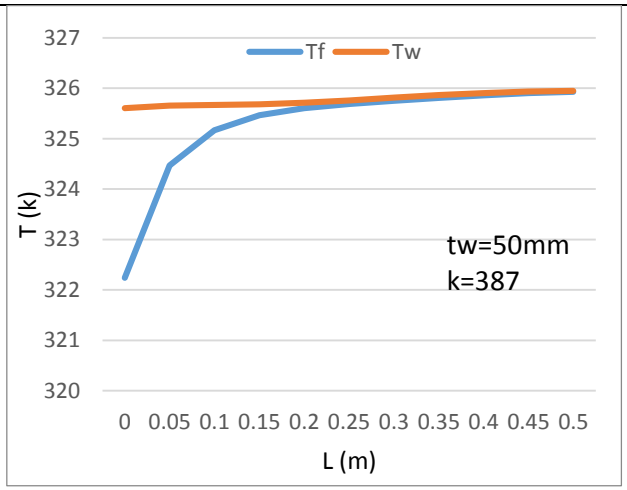

Figure 5: temperature profile along the channel length with different wall thicknesses (1 mm, 5 mm, and 50mm) with the same thermal conductivity of 387 W/m^{2}C

3-2 Wall heat flux and Nusselt number

As mentioned above, the channel wall sets with constant heat flux, but this heat flux does not remain as it is due to the conjugate conduction through the wall thickness. **Fig. 6** shows the heat flux variation along the channel length for different thermal conductivities and wall thicknesses. It is clear that at low conductivity, the heat flux remains constant as it is, but at high conductivity, the heat flux begins with a high value and falls at the trailing edge of the channel. This is also due to the conjugate heat transfer which is opposite to the flow direction. So the conjugate conduction works as a redistributor of the heat flux at the walls.

Fig. 7 shows the local Nusselt number along channel length for different wall conductivities and thicknesses. It shows that the standard or usual behavior of the Nusselt number appears at low thermal conductivity and for small thickness, which is why the conjugate is neglected under these conditions. Also, the conjugate plays as a flattener for the Nusselt number, reducing the effect of the high Nusselt number at the entrance region by redistributing the heat flux at the wall. In terms of the average Nusselt number, **Fig. 8** shows the effect of wall thickness on the average Nusselt number. It can be seen that the average Nusselt number decreased with wall thickness increment, whereas a decrease of 8% when increasing wall thickness from 1 mm to 50 mm for the same thermal conductivity of 10 W/m^{2}C. **Fig. 9** shows the effect of thermal conductivity on the average Nusselt number for the same wall thickness of (1mm); it can be seen an increase in the average Nusselt number with thermal conductivity increment till it reaches a value of 10 W/m^{2}C after which Nusselt number falls. An increase in Nusselt number of 19% with thermal conductivity changes from 0.25 W/m^{2}C to 10 W/m^{2}C. The increase in Nusselt number is due to utilizing of the entrance region effect of high Nusset number by redistributing the heat flux on the wall in a way reducing the bottleneck effect till it reaches a maximum value and then falls at a condition when the heat flux further redistributes made the bottleneck effect returns.

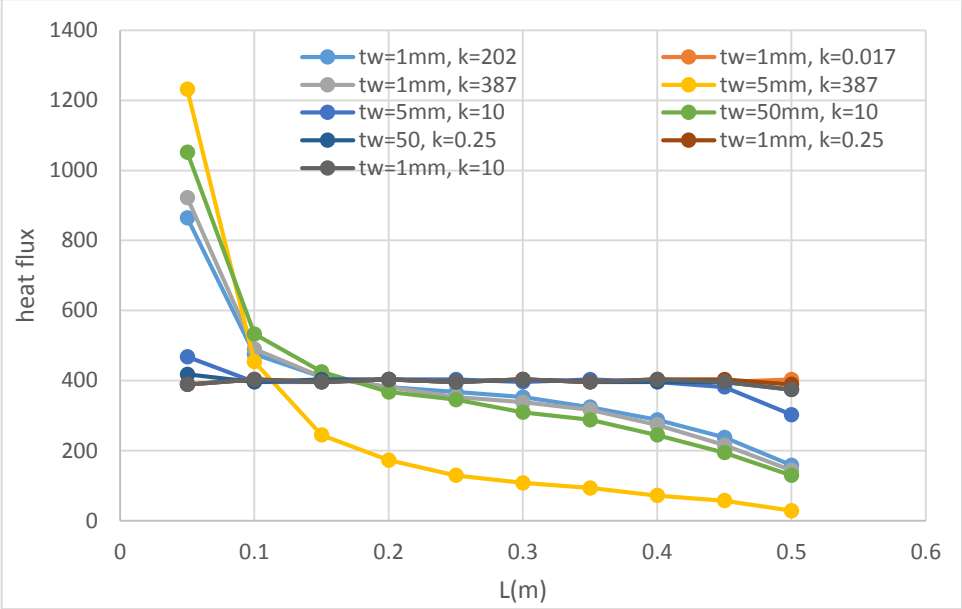

Figure 6. Wall heat flux along channel length for different wall conductivities and thicknesses

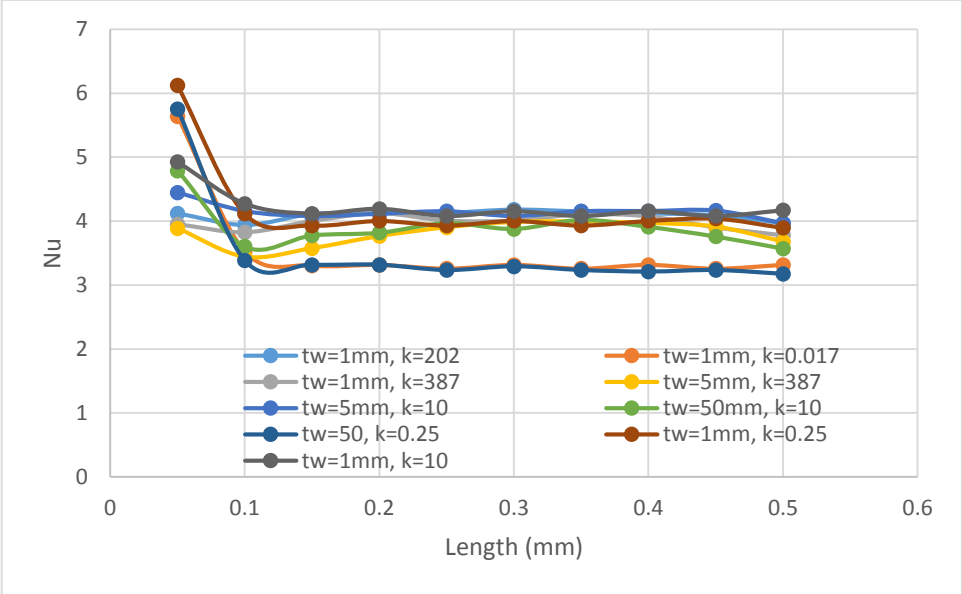

Figure 7. Local Nusselt number along channel length for different wall conductivities and thicknesses

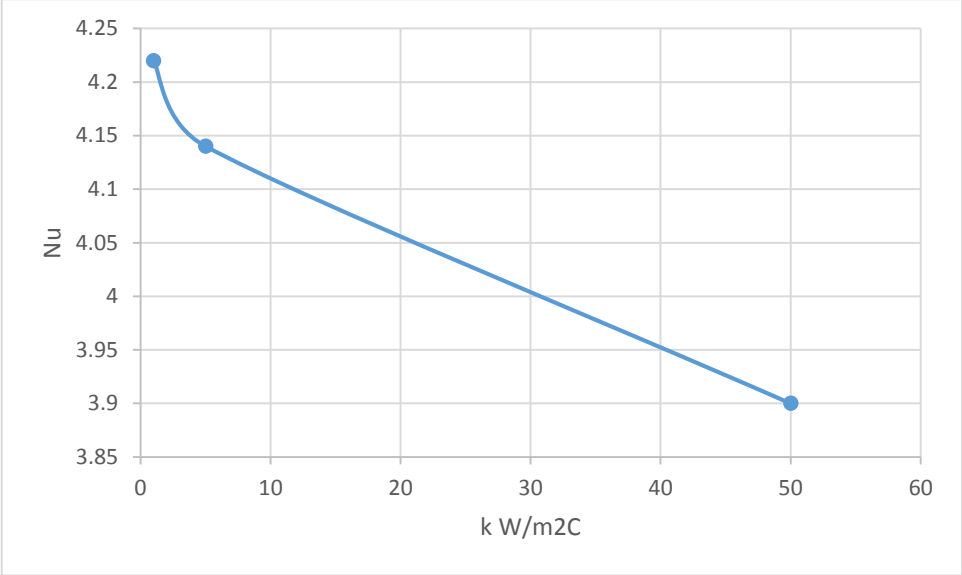

Figure 8. Average Nusselt number versus thermal conductivity for the same wall thickness of 1mm

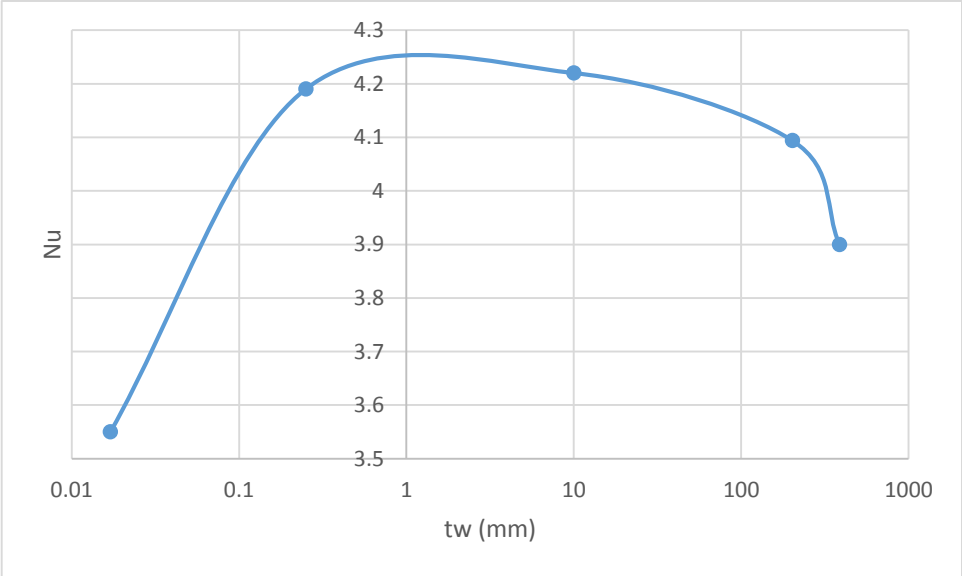

Figure 8. Average Nusselt number versus wall thickness for the same wall thermal conductivity of 10 W/m^{2}C

4. CONCLUSIONS

A numerical investigation was performed to analyze the effect of conjugate heat transfer on laminar airflow in a mini rectangular channel. The influence of two parameters was studied: wall thickness and thermal conductivity. Wall thickness of (1, 5, and 50) mm, while thermal conductivity of (0.25, 10, 202, and 387) W/m^{2}C was chosen. The results show that the conjugate conduction impact appears at high thermal conductivity and for large wall thickness. It

significantly influences the temperature profile along channel length, whereas it flattens the wall temperature profile and curves the fluid temperature profile along the channel length. It also suppresses the entrance region effects by flattening the local Nusselt number and redistributing wall heat flux along the channel wall. There was a decrease in the average Nusselt number of 8% when increasing wall thickness from 1 mm to 50 mm for the same thermal conductivity of 10 W/m^2C, while an increase in Nusselt number of 19% with thermal conductivity changes from 0.25 W/m^2C to 10 W/m^2C was observed.

REFERENCES

- Abdollahzadeh, M., et al., 2017. Assessment of RANS turbulence models for numerical study of laminar-turbulent transition in convection heat transfer, International Journal of Heat and Mass Transfer, 115, pp. 1288–1308
- .
- Ajeena, A.M., and Al-Madhhachi, H.S., 2020. Advanced thermal analysis of three-dimensional conjugate heat transfer with radial radiation in horizontal pipe for sustainability, Journal of Mechanical Engineering Research and Developments, 43(4), pp. 134–149.

- Al-Zaharnah, I.T., Yilbas, B.S., and Hashmi, M.S.J., 2000. Conjugate heat transfer in fully developed laminar pipe flow and thermally induced stresses, Computer Methods in Applied Mechanics and Engineering, 190(8), pp. 1091–1104.

- Arici, M.E., and Aydin, O., 2009. Conjugate heat transfer in thermally developing laminar flow with viscous dissipation effects, Heat and Mass Transfer/Waerme- und Stoffuebertragung, 45(9), pp. 1199–1203.

- Bilir, Ş., 2002. Transient conjugated heat transfer in pipes involving two-dimensional wall and axial fluid conduction, International Journal of Heat and Mass Transfer, 45(8), pp. 1781–1788.

- Canli, E., Ates, A., and Bilir, S., 2018. Conjugate heat transfer for turbulent flow in a thick walled plain pipe, EPJ Web of Conferences, 180, pp. 1–8.

- Carlson, J.-R., 2011. Inflow/Outflow Boundary Conditions with Application to FUN3D, National Aeronautics and Space Administration, (October), pp. 1–38.

- Hajmohammadi, M.R., Rahmani, M., Campo, A., and Joneydi Shariatzadeh, O., 2014. Optimal design of unequal heat flux elements for optimized heat transfer inside a rectangular duct, Energy, 68, pp. 609–616.

- He, J., Juan He, Qinghua D., Weilun Z., Wei H., Tieyu G., Zhenping F., 2020. Conjugate Heat Transfer Characteristics of Double Wall Cooling on a Film Plate With Gradient Thickness, ASME Turbo Expo 2020: Turbomachinery Technical Conference and Exposition.

- Holman, J.P., 2010. *Heat Transfer*, tenth edition.
- Joneydi Shariatzadeh, O., 2016. Analytical solution of conjugate turbulent forced convection boundary layer flow over plates, Thermal Science, 20(5), pp. 1499–1507.
- Karvinen, R., 1978. Some new results for conjugated heat transfer in a flat plate, International Journal of Heat and Mass Transfer, 21(9), pp. 1261–1264.
- Khalesi, J., and Sarunac, N., 2019. Numerical analysis of flow and conjugate heat transfer for supercritical CO2 and liquid sodium in square microchannels, International Journal of Heat and Mass Transfer, 132, pp. 1187–1199.
- Kokugan, T., KINOSHITA, T., TANIGUCHI, N., and SHIMIZU, M., 1975. Natural convection flow rate in a heated vertical tube, Journal of Chemical Engineering of Japan, 8(6), pp. 445–450.
- Kuznetsov, G. V., and Sheremet, M.A., 2010. Turbulent regime of thermogravitational convection in a closed cavity, Journal of Engineering Physics and Thermophysics, 83(2), pp. 346–357.
- Malvandi, A., Hedayati, F., and Ganji, D.D., 2015. Onset of the mutual thermal effects of solid body and nanofluid flow over a flat plate theoretical study, Journal of Applied Fluid Mechanics, 8(4), pp. 835–843.
- Méndez, F., and Treviño, C., 2000. The conjugate conduction-natural convection heat transfer along a thin vertical plate with non-uniform internal heat generation, International Journal of Heat and Mass Transfer, 43(15), pp. 2739–2748.
- Merkin, J.H., and Pop, I., 1996. Conjugate free convection on a vertical surface, International Journal of Heat and Mass Transfer, 39(7), pp. 1527–1534.
- Mohammed, H.A., and Salman, Y.K., 2007. Laminar air flow free convective heat transfer inside a vertical circular pipe with different inlet configurations, Thermal Science, 11(1), pp. 43–63.
- Mohammed, H.A., and Salman, Y.K., 2008. Numerical study of combined convection heat transfer for thermally developing upward flow in a vertical cylinder, Thermal Science, 12(2), pp. 89–102.
- Satish, N., and Venkatasubbaiah, K., 2016. Conjugate heat transfer analysis of turbulent forced convection of moving plate in a channel flow, Applied Thermal Engineering, 100, pp. 987–998.
- Tiselj, I., and Cizelj, L., 2012. DNS of turbulent channel flow with conjugate heat transfer at Prandtl number 0.01, Nuclear Engineering and Design, 253, pp. 153–160.

- Varol, Y., Oztop, H.F., and Koca, A., 2008. Entropy generation due to conjugate natural convection in enclosures bounded by vertical solid walls with different thicknesses, International Communications in Heat and Mass Transfer, 35(5), pp. 648–656.
- Yapici, H., and Albayrak, B., 2004. Numerical solutions of conjugate heat transfer and thermal stresses in a circular pipe externally heated with non-uniform heat flux, Energy Conversion and Management, 45(6), pp. 927–937.